

Dislocation-Based Boundary-Element Method for Crack Problems in Anisotropic Half-Planes

H. Huang* and G. A. Kardomateas†

Georgia Institute of Technology, Atlanta, Georgia 30332-0150

A dislocation-based boundary-element method (BEM) is presented to provide solutions to the crack problems in anisotropic half-planes. The boundary of the half-plane is first modeled by a dislocation array, which is then discretized into boundary elements. Each element is simulated as a continuous dislocation array with linear distribution between the two element nodes. As a result, the singular integral equations derived from the continuous dislocation method for each element can be solved analytically. After the dislocation densities at the element nodes are determined from the prescribed traction forces along the half-plane boundary, the elastic solution of the half-plane can be calculated. Two basic solutions for an anisotropic half plane, that is, traction boundary solution and dislocation solution, are derived and compared with the analytical solutions. These solutions are then applied to solve crack problems in the half-plane subjected to different loading. The results from the dislocation-based BEM are compared with those from the analytical solutions to verify the described BEM. Excellent agreements are achieved for all of the cases.

I. Introduction

THE continuous dislocation technique has been widely used in fracture mechanics to evaluate the crack-tip stress intensity factors. Two basic elastic solutions, the boundary traction solution and the dislocation solution, must be available in order to apply the continuous dislocation method to solve crack problems. Because the number of dislocation solutions for different geometries are limited, the application of the continuous dislocation technique is restricted to well-defined structures and geometries such as infinite plane, half-plane, bimaterial infinite plane, infinite plane with circular inclusion, etc. Several researchers managed to obtain the dislocation solution in either isotropic or orthotropic finite strip by introducing an additional elastic field expressed in Fourier transform.^{1–3} A hybrid boundary-element method (BEM) was proposed by Chandra et al.⁴ and Jiang et al.⁵ to handle the finite geometry. In their studies, the microcracks were simulated by dislocation arrays, whereas the boundary tractions were calculated by conventional BEM. The two solutions were then combined to solve the problem of microscale cracks in macroscale structures. Huang and Kardomateas⁶ presented a method to calculate the dislocation solution in an anisotropic infinite strip, which used a dislocation array to enforce the traction-free conditions at the boundary of the anisotropic strip. This method involves integrations over the infinite straight boundary, and Gaussian quadrature is employed to solve the singular integral equations.

Another application of the continuous dislocation technique that did not get much attention is in solving boundary traction problems. A surface dislocation method was proposed by Jagannadham and Marcinkowski⁷ to calculate the stress fields of a finite body subjected to either applied stresses or internal stresses. Sheng⁸ applied the dislocation distribution method to solve a two-dimensional elastostatics problem with a closed boundary. In his study, the integration over the closed boundary is solved numerically by the Lobatto–Chebyshev formula.⁹

The applications of the continuous dislocation method to both crack problems and boundary-traction problems essentially result in solving a series of singular integral equations. The Gaussian–

Chebyshev method¹⁰ and Lobatto–Chebyshev method⁹ are two most commonly used numerical methods to reduce the singular integral equations into linear algebraic equations. Based on complex potentials, Cheung and Chen¹¹ and Zang and Gudmundson¹² introduced a boundary integral equation method for kinked cracks in infinite planes and half planes.

A dislocation-based BEM is presented in this paper to solve the singular integral equations generated from the formulation of the dislocation solution and the boundary traction solution. Unlike the methods just mentioned, the proposed dislocation-based BEM employs dislocation arrays to solve both the boundary problem and the crack problem. The boundary of the finite body is simulated by boundary elements that have a linear distribution of dislocations between the nodes. The resulting integral equations for each element can be solved analytically, which reduces the complicated integral equations into a problem of solving linear equations. The conventional continuous dislocation method is employed to calculate the mixed-mode stress intensity factors for cracks in an anisotropic half-plane. The dislocation-based BEM has the flexibility to simulate the two surfaces, that is, the boundary and the crack surfaces, with different arrays of dislocations. To take advantage of this, one can assign coarse dislocations along the nonsingular surface such as the boundary surface and the crack surface that is far away from the crack tip and assign dense dislocations close the singular point, for example, the crack tip, and thus reduce the calculation burden required by other conventional finite element methods and BEM approaches. Because of this kind of flexibility, the method is well suited to solve multiscale situations, where the cracks are several orders smaller than the body they reside in.

Even though the present paper deals with the application of the dislocation-based BEM to anisotropic half-planes subjected to boundary traction forces, the proposed BEM approach can be easily extended to solve crack problems in anisotropic finite structures with arbitrary geometries and loadings.

II. Formulation

As shown in Fig. 1, the boundary of a half-plane can be modeled as a dislocation array in an infinite plane. If the traction forces along the x axis in the infinite plane caused by the dislocation array equal the external traction forces applied at the half-plane boundary, then the elastic solution of the upper infinite plane as a result of the dislocations is equivalent to the elastic solution of the half-plane subjected to the prescribed external forces. The idea is very simple; however, it is not an easy task to determine the dislocation distributions along the boundary because the solution usually involves

Received 8 April 2002; revision received 9 September 2003; accepted for publication 12 September 2003. Copyright © 2004 by H. Huang and G. A. Kardomateas. Published by the American Institute of Aeronautics and Astronautics, Inc., with permission. Copies of this paper may be made for personal or internal use, on condition that the copier pay the \$10.00 per-copy fee to the Copyright Clearance Center, Inc., 222 Rosewood Drive, Danvers, MA 01923; include the code 0001-1452/04 \$10.00 in correspondence with the CCC.

*Postdoctoral Fellow, School of Aerospace Engineering.

†Professor, School of Aerospace Engineering, Associate Fellow AIAA.

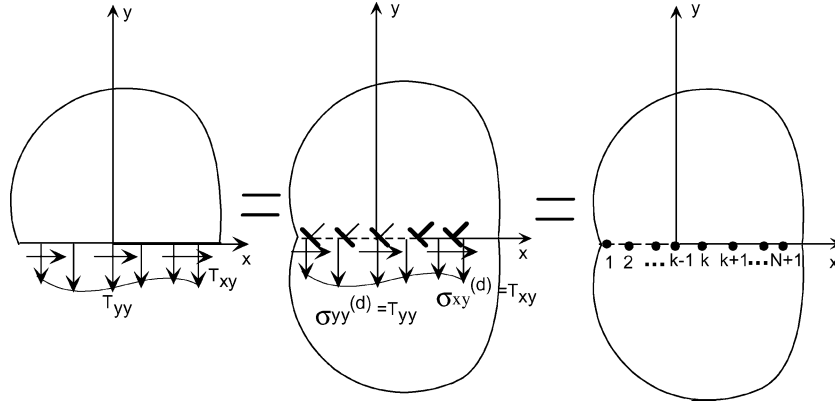


Fig. 1 Simulation of half-plane boundary by dislocation array and boundary elements.

singular integrations from $-\infty$ to ∞ . In this paper, we will present an efficient boundary-element method to overcome the difficulty of solving the singular integral equations.

A. Dislocation Solution in an Anisotropic Infinite Plane

The analytical solution for a dislocation in an anisotropic infinite plane can be found in Lee¹³ and is summarized in Appendix A. The stress components at (x, y) as a result of a dislocation b_m at (x_0, y_0) can be written in real form as

$$\begin{aligned} \sigma_{ij}(x, y) &= f_{mij}(x, y, x_0, y_0)b_m(x_0, y_0) \\ m &= x, y \quad ij = xx, yy, xy \end{aligned} \quad (1)$$

The physical meaning of $f_{mij}(x, y, x_0, y_0)$ are the stress components σ_{ij} at (x, y) as a result of a unit dislocation $b_m(x_0, y_0) = 1$, $m = x, y$ and are expressed as follows:

$$\begin{aligned} f_{mij}(x, y, x_0, y_0) &= \frac{A_{mij}[(x - x_0) + \alpha_1(y - y_0)] + B_{mij}(y - y_0)}{[(x - x_0) + \alpha_1(y - y_0)]^2 + \beta_1^2(y - y_0)^2} \\ &+ \frac{C_{mij}[(x - x_0) + \alpha_2(y - y_0)] + D_{mij}(y - y_0)}{[(x - x_0) + \alpha_2(y - y_0)]^2 + \beta_2^2(y - y_0)^2} \end{aligned} \quad (2)$$

where A_{mij} , B_{mij} , C_{mij} , and D_{mij} are functions of the material constants (Appendix A).

B. Anisotropic Half-Plane Subjected to Boundary Traction Forces

The continuous dislocation method has been used extensively for crack problems in anisotropic domains. In this section, we will apply the dislocation technique to solve another problem, that is, an anisotropic half-plane with prescribed load applied at the boundary. An unknown distribution of dislocations is assigned along the x axis of an infinite plane to simulate the boundary of the half-plane, as shown in Fig. 1. Assuming that the distribution of the dislocation densities is $b_m(t, 0)$ and is continuous from $-\infty$ to ∞ , then the traction forces along the x axis caused by the dislocation array are

$$\sigma_{ij}^{(d)}(x, 0) = \int_{-\infty}^{\infty} f_{mij}(x, 0, t, 0)b_m(t, 0) dt, \quad ij = xy, yy \quad (3)$$

Because the elastic fields of a dislocation in the infinite plane are in self-equilibrium, it is reasonable to assume that the dislocation densities are zero for those portions along the boundary that are far away from the applied traction forces. Thus, the integration can be truncated to an interval $[a, b]$, which depends on the prescribed load. As a result, Eq. (3) can be rewritten as

$$\sigma_{ij}^{(d)}(x, 0) = \int_a^b f_{mij}(x, 0, t, 0)b_m(t, 0) dt, \quad ij = xy, yy \quad (4)$$

To solve the singular integral in Eq. (4), interval $[a, b]$ is discretized into N boundary elements with two nodes at each end, as

shown in Fig. 1. For the boundary element k , the coordinate of the first node is t_k , the second node is t_{k+1} , and the length of the element is $d_k = t_{k+1} - t_k$. The dislocation densities at the first and the second node are denoted as b_m^k and b_m^{k+1} , respectively, and the dislocation distribution along the boundary element is assumed to be linear, that is,

$$b_m(t) = b_m^k \frac{t_{k+1} - t}{d_k} - b_m^{k+1} \frac{t_k - t}{d_k}, \quad t \in [t_k, t_{k+1}] \quad (5)$$

Discretizing the integration equations (4) and substituting into Eq. (5), we obtain

$$\begin{aligned} \sigma_{ij}^{(d)}(x, 0) &= \sum_{k=1}^N \int_{t_k}^{t_{k+1}} f_{mij}(x, 0, t, 0) \\ &\times \left(b_m^k \frac{t_{k+1} - t}{d_k} - b_m^{k+1} \frac{t_k - t}{d_k} \right) dt \\ &= \sum_{k=1}^N [b_m^k I_{mij}^{k,k}(x, 0) + b_m^{k+1} I_{mij}^{k,k+1}(x, 0)] \quad ij = xy, yy \end{aligned} \quad (6)$$

where

$$I_{mij}^{k,k}(x, 0) = \int_{t_k}^{t_{k+1}} f_{mij}(x, 0, t, 0) \frac{t_{k+1} - t}{d_k} dt \quad (7a)$$

$$I_{mij}^{k,k+1}(x, 0) = - \int_{t_k}^{t_{k+1}} f_{mij}(x, 0, t, 0) \frac{t_k - t}{d_k} dt \quad (7b)$$

The first superscript of $I_{mij}^{k,k+1}$ represents the k th boundary element, and the second superscript represents the $(k+1)$ th node. The solutions for these two singular integrations are analytical and are given in Appendix B.

The unknown dislocation densities at the nodes b_m^k , $k = 1, \dots, N+1$ are determined from the prescribed load T_{ij} along the half plane boundary, that is,

$$\begin{aligned} \sigma_{ij}^{(d)}(x, 0) &= \sum_{k=1}^N [b_m^k I_{mij}^{k,k}(x, 0) + b_m^{k+1} I_{mij}^{k,k+1}(x, 0)] = T_{ij}(x, 0) \\ &ij = xy, yy \end{aligned} \quad (8)$$

Expressing Eq. (8) in matrix form, we have

$$\begin{bmatrix} A_{xxy}(l, k) & A_{yyx}(l, k) \\ A_{xyy}(l, k) & A_{yyy}(l, k) \end{bmatrix} \begin{Bmatrix} b_x^k \\ b_y^k \end{Bmatrix} = \begin{Bmatrix} T_{xy}(x_l, 0) \\ T_{yy}(x_l, 0) \end{Bmatrix} \quad k = 1, 2, \dots, N+1 \quad (9)$$

where x_l are the collocation points. In this study, two collocation are chosen for each boundary element, that is,

$$x_{2k-1} = t_k + d_k/4, \quad x_{2k} = t_{k+1} - d_k/4, \quad d_k = t_{k+1} - t_k$$

$$k = 1, 2, \dots, N \quad (10)$$

$$A_{mij}(l, 1) = I_{mij}^{1,1}(x_l, 0) \quad (11a)$$

$$A_{mij}(l, h) = I_{mij}^{h-1,h}(x_l, 0) + I_{mij}^{h,h}(x_l, 0)$$

$$h = 2, 3, \dots, N \quad (11b)$$

$$A_{mij}(l, N+1) = I_{mij}^{N,N+1}(x_l, 0) \quad (11c)$$

The dislocation density at each node is determined from Eq. (9) as

$$\begin{Bmatrix} b_x^k \\ b_y^k \end{Bmatrix} = (A^T \times A)^{-1} A^T \times \begin{Bmatrix} T_{xy}(x_l, 0) \\ T_{yy}(x_l, 0) \end{Bmatrix} \quad (12)$$

The stress components at point (x, y) in the upper infinite plane as a result of the dislocations can be calculated as

$$\sigma_{ij}(x, y) = \int_a^b f_{mij}(x, y, t, 0) b_m(t, 0) dt$$

$$= \sum_{k=1}^N [b_m^k I_{mij}^{k,k}(x, y) + b_m^{k+1} I_{mij}^{k,k+1}(x, y)] \quad (13)$$

which are equivalent to the stress components in the half-plane as a result of the prescribed traction forces $T_{ij}(x, 0)$.

C. Dislocation Solution in an Anisotropic Half-Plane

The elastic fields of a dislocation in an anisotropic half-plane can be decomposed into two elastic fields in an infinite plane, as shown in Fig. 2. The first one is an infinite plane with a single dislocation located at (x_0, y_0) , and the dislocation generates residual stresses $\sigma_{ij}^{(s)}(x, 0)$, $ij = xy, yy$ along the x axis. The second infinite plane is subjected to traction forces along the x axis that are the opposite of the residual stresses in the first infinite plane. When we superimpose these two infinite planes together, the traction forces along the x axis cancel out, and the elastic fields of the upper infinite plane are equivalent to the elastic fields of a dislocation in an anisotropic half-plane. Thus, the elastic solution for a dislocation in an anisotropic half-plane is the superposition of the solutions presented in Secs. II.A and II.B, that is,

$$\sigma_{ij}(x, y) = f_{mij}(x, y, x_0, y_0) b_m(x_0, y_0)$$

$$+ \sum_{k=1}^N [b_{nm}^k I_{nij}^{k,k}(x, y) + b_{nm}^{k+1} I_{nij}^{k,k+1}(x, y)] \quad (14)$$

where b_{nm}^k are related to the single dislocation $b_m(x_0, y_0)$ and are calculated from the residual traction forces along the x axis. Substituting

$$T_{ij}(x_l, 0) = -\sigma_{ij}^{(s)}(x_l, 0) = -f_{mij}(x_l, 0, x_0, y_0) b_m(x_0, y_0)$$

$$ij = xy, yy \quad (15)$$

into Eq. (12), we obtain

$$\begin{Bmatrix} b_{xm}^k \\ b_{ym}^k \end{Bmatrix} = -(A^T \times A)^{-1} A^T \times \begin{Bmatrix} f_{mxy}(x_l, 0, x_0, y_0) b_m(x_0, y_0) \\ f_{myy}(x_l, 0, x_0, y_0) b_m(x_0, y_0) \end{Bmatrix} \quad (16)$$

Because of the linearity of the elastic fields of a dislocation, we can express b_{nm}^k as

$$b_{nm}^k(x_l, 0, x_0, y_0) = \tilde{b}_{nm}^k(x_l, 0, x_0, y_0) b_m(x_0, y_0)$$

$$n = x, y, \quad m = x, y \quad (17)$$

The physical meaning of \tilde{b}_{nm}^k are the dislocation densities b_n^k , $n = x, y$ at the k th boundary-element nodes caused by a unit dislocation $b_m(x_0, y_0) = 1$, $m = x, y$. Setting $b_x = 1$ in Eq. (17), we have

$$\begin{Bmatrix} \tilde{b}_{xx}^k \\ \tilde{b}_{yx}^k \end{Bmatrix} = -(A^T \times A)^{-1} A^T \times \begin{Bmatrix} f_{xxy}(x_l, 0, x_0, y_0) \\ f_{xyy}(x_l, 0, x_0, y_0) \end{Bmatrix} \quad (18a)$$

Similarly,

$$\begin{Bmatrix} \tilde{b}_{xy}^k \\ \tilde{b}_{yy}^k \end{Bmatrix} = -(A^T \times A)^{-1} A^T \times \begin{Bmatrix} f_{yxy}(x_l, 0, x_0, y_0) \\ f_{yyy}(x_l, 0, x_0, y_0) \end{Bmatrix} \quad (18b)$$

The elastic fields of a single dislocation in an anisotropic half-plane can thus be expressed as

$$\sigma_{ij}(x, y) = \tilde{f}_{mij}(x, y, x_0, y_0) b_m(x_0, y_0) \quad (19)$$

where

$$\tilde{f}_{mij}(x, y, x_0, y_0) = f_{mij}(x, y, x_0, y_0)$$

$$+ \sum_{k=1}^N [b_{nm}^k I_{nij}^{k,k}(x, y) + b_{nm}^{k+1} I_{nij}^{k,k+1}(x, y)] \quad (20)$$

D. Applying Dislocation Solution to Crack Problems in Anisotropic Half-Planes

Based on the implementation of Bueckner's¹⁴ theorem, an anisotropic half-plane with a crack subjected to traction forces can be decomposed into two half-planes without a crack, as shown in Fig. 3. In the first half-plane, the crack is replaced by a dislocation array, and the boundary is free of traction forces. The second half-plane is simply a perfect half-plane subjected to external traction forces. The dashed line stands for the location of the crack.

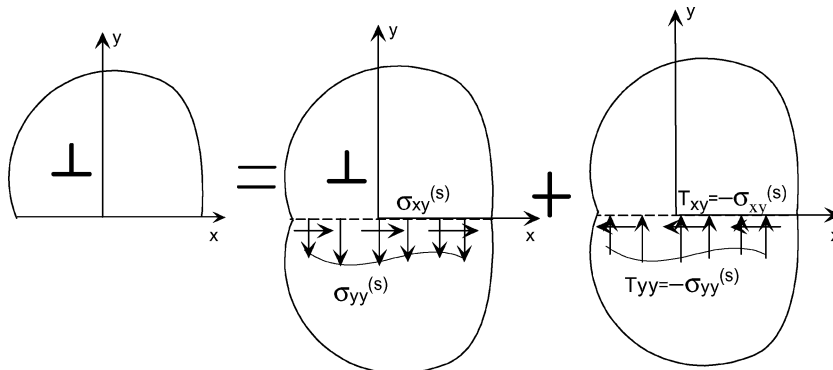


Fig. 2 Single dislocation in a half-plane as a superposition of two infinite planes.

To satisfy the crack surface traction-free conditions, the dislocation densities in the first half-plane should be determined such that the traction forces along the dashed line caused by the dislocation array should cancel out the traction forces along the dashed line as a result of the external tractions in the second half-plane. The crack-tip stress intensity factors can then be calculated from the dislocation densities at the crack tip. As the dislocation solution and the boundary traction solution for an anisotropic half-plane have been derived in the preceding two sections, the procedure to solve the crack problems are conventional. Interested readers can refer to Hill et al.¹⁵ and Huang and Kardomateas.⁶

III. Results and Discussion

This paper is intended to describe a new dislocation-based BEM. Anisotropic half-plane is chosen to study here because both the analytical boundary traction solution and dislocation solution in an anisotropic half-plane are known. All of the results obtained using the dislocation-based BEM are compared with the analytical solutions to verify this method.

A. Elastic Fields of an Anisotropic Half-Plane Subjected to Boundary Traction Forces

The example we studied in this section is an anisotropic half-plane with a moment applied at the boundary, as shown in Fig. 4. The material is a typical graphite/epoxy unidirectional fiber-reinforced composite with elastic constants: $E_L = 170.65$ GPa, $E_T = 55.6$ GPa, $G_{LT} = 4.83$ GPa, and $\mu_{LT} = 0.1114$, where L and T are the directions parallel and perpendicular to the fibers, respectively. The fiber direction is aligned with the x axis that is, fiber orientation $\theta = 0$. A moment $M = 1$ is simulated by a linear distributed load applied from $p = -1$ to $q = 1$; thus, the traction forces along the boundary are

$$T_{yy}(t, 0) = 3M/(q^3 - p^3)[t - (p + q)/2]$$

for $t \in [p, q]$, $T_{yy}(t, 0) = 0$, otherwise (21a)

$$T_{xy}(t, 0) = 0, \quad t \in [-\infty, \infty] \quad (21b)$$

The comparison of results from dislocation-based BEM and the analytical solution¹⁶ are shown in Fig. 5. N is the total number of boundary elements. Obviously, we achieved a very good agreement between these two groups of results.

B. Elastic Fields of an Anisotropic Half-Plane with a Dislocation

The stress components σ_{yy} in an anisotropic half-plane because of a dislocation located at $x_0 = 0$, $y_0 = 0.5$ are listed in Table 1. Here we compare the results from different meshing with the analytical solution as well as the results from solving the singular integral equations (4) by Gaussian quadrature.⁶ The integral interval $[a, b]$ in Eqs. (4) is chosen to be $[-50, 50]$. Three different meshings are implemented. The first one is uniformly distributed boundary elements along the boundary, that is, all of the boundary elements have the same length. The second one is to divide the interval $[-50, 50]$ into six subintervals $[-50, -10]$, $[-10, -5]$, $[-5, 0]$, $[0, 5]$, $[5, 10]$, and $[10, 50]$, and each subinterval is then discretized into $N/6$ boundary elements, where N is the total number of boundary elements.

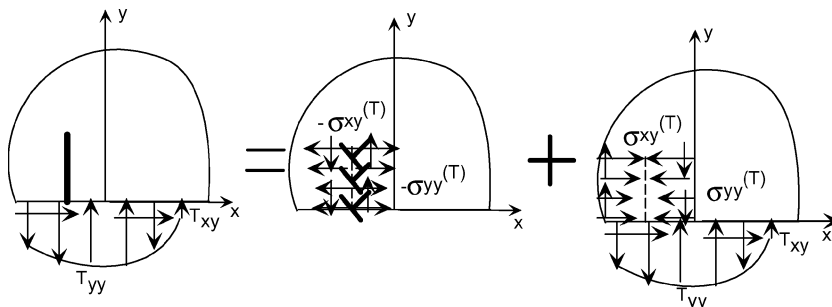


Fig. 3 Application of Bueckner's principle.

The third meshing is similar to the second one except that the six subintervals are $[-50, -10]$, $[-10, -2]$, $[-2, 0]$, $[0, 2]$, $[2, 10]$, and $[10, 50]$. Because the residual traction forces caused by the dislocation are concentrated around $x = 0$ and decay rapidly as $|x|$ increases (Fig. 6), the third meshing is the best as the elements around $x = 0$ are shorter and can simulate the residual traction forces better than other methods. For the Gaussian quadrature method, the dislocation points and the collocation points are calculated from a given formula.^{6,15} Because most of the dislocation points are distributed near the two ends of the interval and less points around $x = 0$, more nodes are required to achieve the same accuracy. (N in Table 1 for Gaussian method is the total number of dislocation points.) We can draw the conclusion here that the dislocation-based BEM is more flexible and efficient because we can adjust the locations of the dislocation and collocation points according to the external traction forces.

C. Crack Problems in an Anisotropic Half-Plane

The first example we studied is that of a half-plane with an edge crack perpendicular to the boundary. The crack surface is loaded with uniform tensile stress σ , as shown in Fig. 7. Table 2 is a list of normalized stress intensity factors (SIF) for a crack of length $a = 5$. The SIFs are normalized as $\bar{K}_I = K_I/\sigma\sqrt{\pi a}$. The boundary is discretized symmetrically about the y axis, and only the meshing of the positive half boundary is shown in Fig. 7. Also, $t = \pm L$ are the cutoff points of the integral in Eq. (4), and L_1 and L_2 are the lengths of the first two subintervals and $L_3 = L - L_1 - L_2$ is the length of the third subinterval. The total number of elements for the positive half-boundary is N , and N_1 and N_2 are the total numbers of elements in

Table 1 Stress components $\sigma_{yy}(x, y)$ in an anisotropic half-plane caused by a dislocation $b_x = 1$ at $x_0 = 0$ and $y_0 = 0.5$

x	y	Analytical	Gaussian,	Meshing 1,	Meshing 2,	Meshing 3,
			$N = 700$	$N = 250$	$N = 120$	$N = 120$
0.1	0.5	-2.1981	-2.1874	-2.1792	-2.1174	-2.1956
0.5	0.5	-0.3584	-0.3976	-0.3347	-0.3231	-0.3593
1.5	0.5	0.2033	0.2179	0.2047	0.2034	0.2032
2.5	0.5	0.1724	0.1649	0.1727	0.1724	0.1724
3.5	0.5	0.1156	0.1202	0.1157	0.1156	0.1156
4.5	0.5	0.0741	0.0711	0.0741	0.0741	0.0741

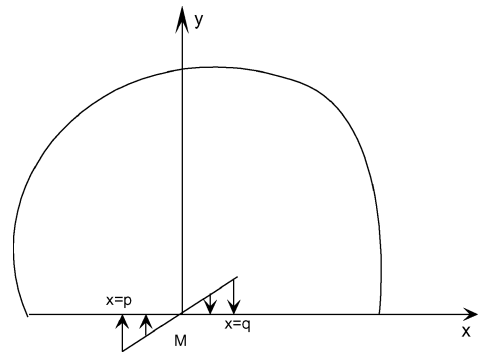


Fig. 4 Half-plane with bending moment applied at the center.

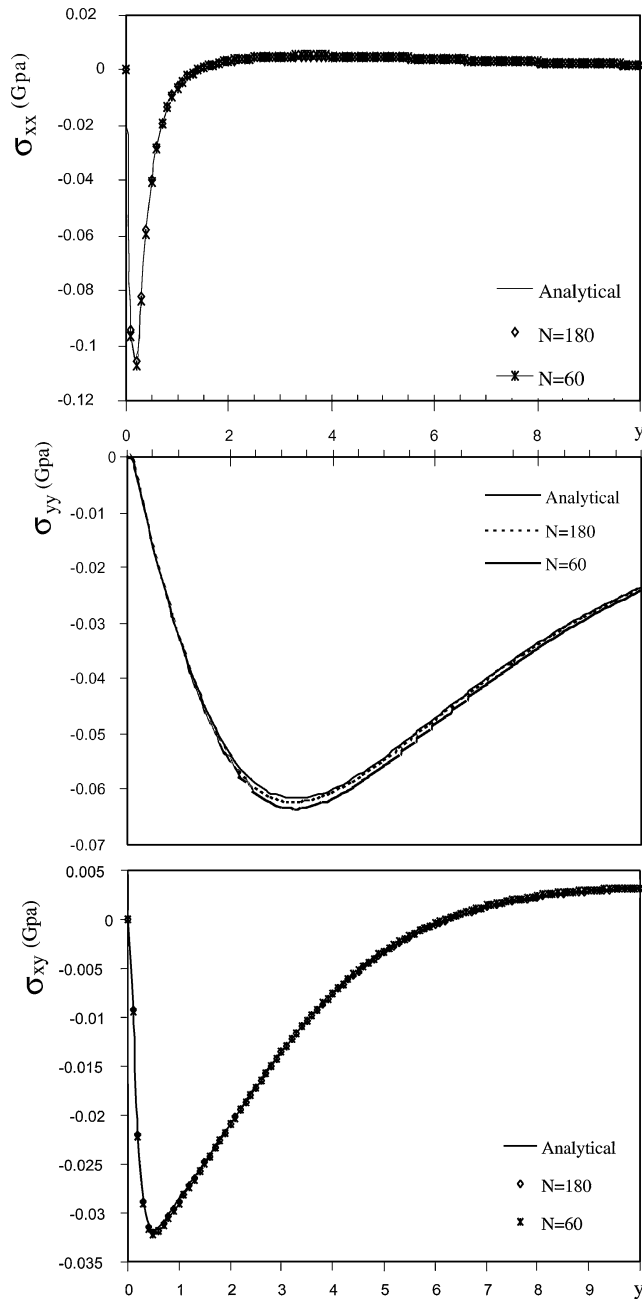


Fig. 5 Comparison of the stress components for a half-plane subjected to a bending moment at the origin. The stress points are located at $x = 2$; y is the variable.

subintervals 1 and 2, respectively. The analytical SIF is calculated from the analytical dislocation solution. The errors between the SIFs from the boundary-element method and the analytical method are less than 4% for all meshing schemes. Furthermore, where the integral is truncated has a slight effect on the SIF. For $L = 100$, a total of 50 elements in the positive half-boundary is adequate to achieve accurate results.

In the second example, the half-plane is subjected to two symmetric bending moments M at a distance d from the edge crack (see Fig. 8). The fiber orientation is chosen to be 45 deg. Unlike the first example, we need two elastic solutions to solve the second crack problem. As shown in Fig. 8, the moment $M = 1$ are simulated as a linear stress distribution. Denoting the traction forces along the crack line as a result of the right moment as σ_{ij}^r and those as a result of the left moment as σ_{ij}^l , the traction forces along the crack line as a result of these two moments are $\sigma_{ij} = \sigma_{ij}^l + \sigma_{ij}^r$. The calculation of σ_{ij}^r and σ_{ij}^l is similar to what was described in Sec. III.A by shifting the origin of the coordinate system to the center point of the moment. Because

Table 2 Normalized mode-I SIF for an edge crack of length $a = 5$ in a half-plane^a

Meshing	N_1	N_2	N	L_1	L_2	L	\bar{K}_I	Error, %
1	10	10	50	1	5	60	1.0742	3.19
2	10	20	50	1	9	60	1.0741	3.19
3	20	20	50	2	8	80	1.0604	1.86
4	20	20	70	2	8	80	1.0606	1.88
5	20	20	50	2	8	100	1.0538	1.23
6	30	30	100	2	8	100	1.0539	1.24
Analytical							1.041	

^aThe crack surface is loaded with uniform tensile stresses σ , and the fiber orientation $\theta = 0$ deg.

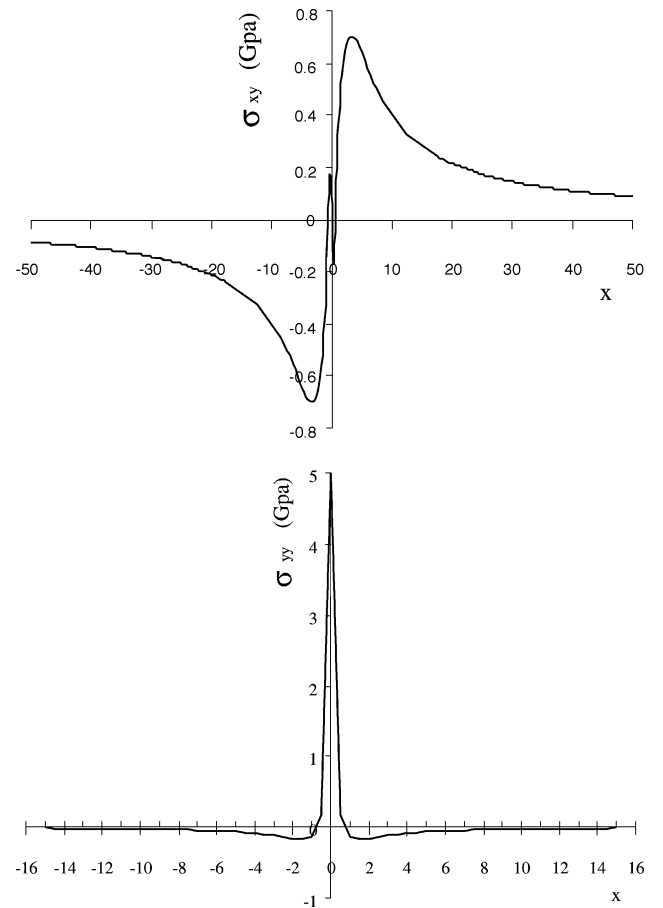


Fig. 6 Residual stresses σ_{xy} and σ_{yy} along the x axis caused by a single dislocation $b_x = 1$ located at $x_0 = 0$ and $y_0 = 0.5$.

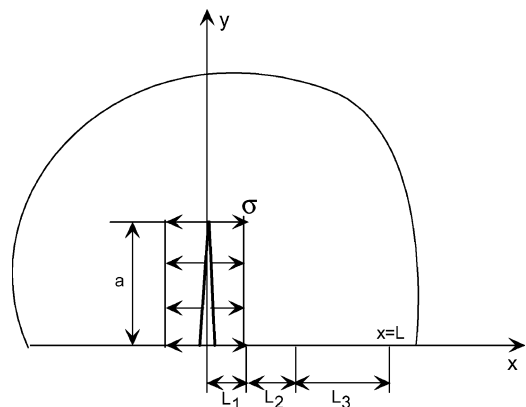


Fig. 7 Half-plane with an edge crack subjected to uniform loading at the crack surface.

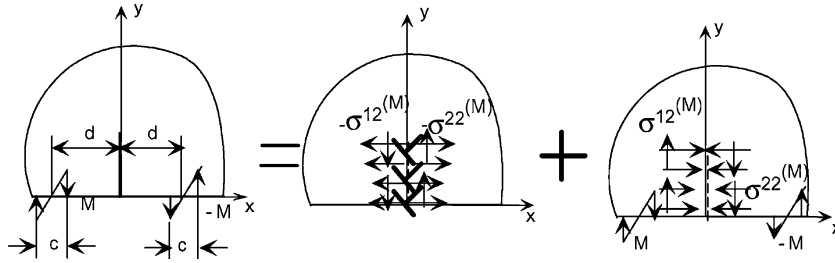


Fig. 8 Half-plane with an edge crack subjected to two symmetric bending moments at the boundary.

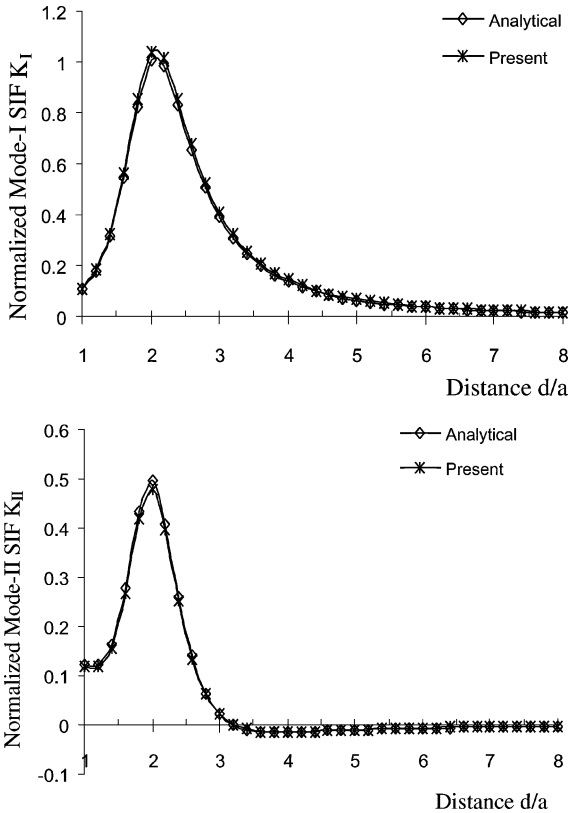


Fig. 9 Normalized mode-I and mode-II SIF for an edge crack in a half-plane subjected to two symmetric bending moments, where a is the crack length and d is the distance between the moment and the crack. Fiber orientation $\theta = 45$ deg.

the distribution of the applied moment and the residual stresses caused by the dislocations along the half-plane boundary are quite different, two different meshings are used. For the dislocation solution, $N_1 = 20$, $N_2 = 20$, $N = 70$, and $L_1 = 2$, $L_2 = 8$, $L = 100$. Because the span of the moment $c = 0.2$, we choose $L_1 = 0.1$, $L_2 = 0.9$, $L = 5$, and $N_1 = 30$, $N_2 = 30$, $N = 100$ for the second solution in Fig. 8. In Fig. 9, we compare the normalized mixed-mode SIFs calculated from the BEM with those from the analytical solutions. Again, the dislocation-based BEM yields very good results.

IV. Conclusions

The presented results indicate that the dislocation-based BEM is very accurate and efficient in providing solutions to crack problems in anisotropic half-planes. This method can be extended to study crack problems in anisotropic finite domains with arbitrary boundary tractions.

Appendix A: Dislocation Solution in Anisotropic Infinite Plane

Let us consider a state of plane strain, that is, $\epsilon_{zz} = \gamma_{yz} = \gamma_{xz} = 0$. In this case, the stress-strain relations for the anisotropic body are¹⁷

$$\begin{bmatrix} \epsilon_{xx} \\ \epsilon_{yy} \\ \epsilon_{zz} \\ \gamma_{xy} \end{bmatrix} = \begin{bmatrix} a_{11} & a_{12} & a_{13} & a_{16} \\ a_{12} & a_{22} & a_{23} & a_{26} \\ a_{13} & a_{23} & a_{33} & a_{26} \\ a_{16} & a_{26} & a_{36} & a_{66} \end{bmatrix} \begin{bmatrix} \sigma_{xx} \\ \sigma_{yy} \\ \sigma_{zz} \\ \tau_{xy} \end{bmatrix} \quad (A1a)$$

where a_{ij} are the compliance constants. (We have used the notation $1 \equiv x$, $2 \equiv y$, $3 \equiv z$, and $6 \equiv xy$.)

Using the condition of plane strain, which requires that $\epsilon_{zz} = 0$, allows elimination of σ_{zz} , that is,

$$\sigma_{zz} = -1/a_{33}(a_{13}\sigma_{xx} + a_{23}\sigma_{yy}) \quad (A1b)$$

Equation (A1a) can then be written in the form

$$\begin{bmatrix} \epsilon_{xx} \\ \epsilon_{yy} \\ \gamma_{xy} \end{bmatrix} = \begin{bmatrix} c_{11} & c_{12} & c_{16} \\ c_{12} & c_{22} & c_{26} \\ c_{16} & c_{26} & c_{66} \end{bmatrix} \begin{bmatrix} \sigma_{xx} \\ \sigma_{yy} \\ \tau_{xy} \end{bmatrix} \quad (A1c)$$

where

$$c_{ij} = a_{ij} - \frac{a_{i3}a_{j3}}{a_{33}} \quad (i, j = 1, 2, 6) \quad (A1d)$$

Problems of this type can be formulated in terms of two complex analytic functions $\phi_k(z_k)$ ($k = 1, 2$) of the complex variables $z_k = x + \mu_k y$, where $\mu_k = \alpha_k + i\beta_k$, $\bar{\mu}_k = \alpha_k - i\beta_k$, $k = 1, 2$ are the roots of the algebraic equation:

$$b_{11}\mu^4 - 2b_{16}\mu^3 + (2b_{12} + b_{66})\mu^2 - 2b_{26}\mu + b_{22} = 0 \quad (A2)$$

It was proven by Lekhnitskii¹⁷ that these roots $\mu_1, \mu_2, \bar{\mu}_1, \bar{\mu}_2$ are either complex or purely imaginary, that is, Eq. (A2) cannot have real roots. Here, μ_1 and μ_2 are chosen to be the ones with positive imaginary parts.

The stress and displacement components can be expressed in terms of $\Phi_k(z_k)$ as¹⁷

$$\sigma_{xx} = 2Re[\mu_1^2\phi_1'(z_1) + \mu_2^2\phi_2'(z_2)] \quad (A3a)$$

$$\sigma_{yy} = 2Re[\phi_1'(z_1) + \phi_2'(z_2)] \quad (A3b)$$

$$\tau_{xy} = -2Re[\mu_1\phi_1'(z_1) + \mu_2\phi_2'(z_2)] \quad (A3c)$$

Now, the complex stress potentials at a point $z = x + iy$ as a result of a single dislocation at $z_0 = x_0 + iy_0$ in an anisotropic infinite plane are given by Lee.¹³ Only the results are presented here.

The derivatives of the complex stress potentials at z as a result of a dislocation at z_0 are given as

$$\phi_1'(z_1, z_0) = \frac{A_1}{z_1 - z_{10}} \quad (A4a)$$

$$\phi_2'(z_2, z_0) = \frac{A_2}{z_2 - z_{20}} \quad (A4b)$$

where

$$z_k = x + \mu_k y = (x + \alpha_k y) + i\beta_k y, \quad k = 1, 2 \quad (A5)$$

A_j constitute the solution of the following equations:

$$\begin{bmatrix} \delta_1 & -\bar{\gamma}_1 & \delta_2 & -\bar{\gamma}_2 \\ -\gamma_1 & \bar{\delta}_1 & -\gamma_2 & \bar{\delta}_2 \\ p(\mu_1) & -p(\bar{\mu}_1) & p(\mu_2) & -p(\bar{\mu}_2) \\ -\bar{p}(\mu_1) & \bar{p}(\bar{\mu}_1) & -\bar{p}(\mu_2) & \bar{p}(\bar{\mu}_2) \end{bmatrix} \begin{bmatrix} A_1 \\ \bar{A}_1 \\ A_2 \\ \bar{A}_2 \end{bmatrix} = \begin{bmatrix} 0 \\ 0 \\ b/2\pi i \\ -\bar{b}/2\pi i \end{bmatrix} \quad (A6a)$$

where

$$p(\mu_k) = (b_{12} - b_{16}\mu_k + b_{11}\mu_k^2) + i(b_{22} - b_{26}\mu_k + b_{12}\mu_k^2)/\mu_k$$

$$\text{and } \bar{p}(\mu_k) = \overline{p(\mu_k)} \quad (A6b)$$

$$b = b_x + ib_y, \quad \gamma_k = 1 - i\mu_k, \quad \delta_k = 1 + i\mu_k \quad k = 1, 2 \quad (A6c)$$

Let us denote the solution of Eqs. (A6) as A_{1x} and A_{2x} for $b = b_x = 1$ and A_{1y} and A_{2y} for $b = i$, that is, $b_y = 1$. According to the physical meaning of $f_{mij}(x, y, x_0, y_0)$, we have

$$f_{xxx} = 2Re\left(\mu_1^2 \frac{A_{1x}}{z_1 - z_{10}} + \mu_2^2 \frac{A_{2x}}{z_2 - z_{20}}\right)$$

$$= 2Re\left\{\mu_1^2 A_{1x} \frac{(x - x_0) + \alpha_1(y - y_0) - i\beta_1(y - y_0)}{[(x - x_0) + \alpha_1(y - y_0)]^2 + \beta_1^2(y - y_0)^2}\right.$$

$$\left. + \mu_2^2 A_{2x} \frac{(x - x_0) + \alpha_2(y - y_0) - i\beta_2(y - y_0)}{[(x - x_0) + \alpha_2(y - y_0)]^2 + \beta_2^2(y - y_0)^2}\right\}$$

$$= \frac{A_{xxx}[(x - x_0) + \alpha_1(y - y_0)] + B_{xxx}(y - y_0)}{[(x - x_0) + \alpha_1(y - y_0)]^2 + \beta_1^2(y - y_0)^2}$$

$$+ \frac{C_{xxx}[(x - x_0) + \alpha_2(y - y_0)] + D_{xxx}(y - y_0)}{[(x - x_0) + \alpha_2(y - y_0)]^2 + \beta_2^2(y - y_0)^2} \quad (A7)$$

where

$$A_{xxx} = 2Re(\mu_1^2 A_{1x}), \quad B_{xxx} = 2Im(\mu_1^2 A_{1x} \beta_1) \quad (A8a)$$

$$C_{xxx} = 2Re(\mu_2^2 A_{2x}), \quad D_{xxx} = 2Im(\mu_2^2 A_{2x} \beta_2) \quad (A8b)$$

Similarly,

$$A_{yxx} = 2Re(\mu_1^2 A_{1y}), \quad B_{yxx} = 2Im(\mu_1^2 A_{1y} \beta_1) \quad (A9a)$$

$$C_{yxx} = 2Re(\mu_2^2 A_{2y}), \quad D_{yxx} = 2Im(\mu_2^2 A_{2y} \beta_2) \quad (A9b)$$

$$A_{xxy} = -2Re(\mu_1 A_{1x}), \quad B_{xxy} = -2Im(\mu_1 A_{1x} \beta_1) \quad (A9c)$$

$$C_{xxy} = -2Re(\mu_2 A_{2x}), \quad D_{xxy} = -2Im(\mu_2 A_{2x} \beta_2) \quad (A9d)$$

$$A_{yyx} = -2Re(\mu_1 A_{1y}), \quad B_{yyx} = -2Im(\mu_1 A_{1y} \beta_1) \quad (A9e)$$

$$C_{yyx} = -2Re(\mu_2 A_{2y}), \quad D_{yyx} = -2Im(\mu_2 A_{2y} \beta_2) \quad (A9f)$$

$$A_{xyy} = 2Re(A_{1x}), \quad B_{xyy} = 2Im(A_{1x} \beta_1) \quad (A9g)$$

$$C_{xyy} = 2Re(A_{2x}), \quad D_{xyy} = 2Im(A_{2x} \beta_2) \quad (A9h)$$

$$A_{yyy} = 2Re(A_{1y}), \quad B_{yyy} = 2Im(A_{1y} \beta_1) \quad (A9i)$$

$$C_{yyy} = 2Re(A_{2y}), \quad D_{yyy} = 2Im(A_{2y} \beta_2) \quad (A9j)$$

Appendix B: Analytical Solution for Integral $I_{mij}^{k,k}(x, y)$

The integrals $I_{mij}^{k,k}(x, y)$ in Eqs. (7) and (13) are defined as

$$I_{mij}^{k,k}(x, y) = \int_{t_k}^{t_{k+1}} f_{mij}(x, y, t, 0) \frac{t_{k+1} - t}{d_k} dt \quad (B1)$$

Substituting Eq. (2) into Eq. (B1) gives

$$I_{mij}^{k,k}(x, y) = \int_{t_k}^{t_{k+1}} \frac{A_{mij}[(x - t) + \alpha_1 y] + B_{mij} y}{[(x - t) + \alpha_1 y]^2 + \beta_1^2 y^2} \times \frac{t_{k+1} - t}{d_k} dt$$

$$+ \int_{t_k}^{t_{k+1}} \frac{C_{mij}[(x - t) + \alpha_2 y] + D_{mij} y}{[(x - t) + \alpha_2 y]^2 + \beta_2^2 y^2} \times \frac{t_{k+1} - t}{d_k} dt \quad (B2)$$

Because the first and second integrals in Eq. (B2) have the same integration form, only the first integral is derived in detail here:

$$I = \int_{t_k}^{t_{k+1}} \frac{A_{mij}[(x - t) + \alpha_1 y] + B_{mij} y}{[(x - t) + \alpha_1 y]^2 + \beta_1^2 y^2} \times \frac{t_{k+1} - t}{d_k} dt$$

$$= \int_{t_k}^{t_{k+1}} \frac{A_{mij}[(x - t) + \alpha_1 y] + B_{mij} y}{[(x - t) + \alpha_1 y]^2 + \beta_1^2 y^2}$$

$$\times \frac{t_{k+1} + (x - t + \alpha_1 y) - x - \alpha_1 y}{d_k} dt \quad (B3)$$

Introducing a change of variable $\xi = x - t + \alpha_1 y$, we have

$$I = - \int_{x - t_k + \alpha_1 y}^{x - t_{k+1} + \alpha_1 y} \frac{A_{mij} \xi + B_{mij} y}{\xi^2 + \beta_1^2 y^2} \times \frac{\xi + (t_{k+1} - x - \alpha_1 y)}{d_k} d\xi$$

$$= -\frac{1}{d_k} \left\{ A_{mij} \int_{x - t_k + \alpha_1 y}^{x - t_{k+1} + \alpha_1 y} \frac{\xi^2}{\xi^2 + \beta_1^2 y^2} d\xi \right.$$

$$\left. + [A_{mij}(t_{k+1} - x - \alpha_1 y) + B_{mij} y] \right.$$

$$\times \int_{x - t_k + \alpha_1 y}^{x - t_{k+1} + \alpha_1 y} \frac{\xi}{\xi^2 + \beta_1^2 y^2} d\xi + B_{mij} y(t_{k+1} - x - \alpha_1 y)$$

$$\left. \times \int_{x - t_k + \alpha_1 y}^{x - t_{k+1} + \alpha_1 y} \frac{1}{\xi^2 + \beta_1^2 y^2} d\xi \right\} \quad (B4)$$

The solutions for the three integrals in Eq. (B4) are

$$\int \frac{\xi^2}{\xi^2 + a} d\xi = \begin{cases} \xi - \sqrt{a} \tan^{-1}\left(\frac{\xi}{\sqrt{a}}\right), & \text{for } a > 0 \\ \xi, & \text{for } a = 0 \end{cases} \quad (B5a)$$

$$\int \frac{\xi}{\xi^2 + a} d\xi = \frac{1}{2} \ln(\xi^2 + a) \quad (B5b)$$

$$\int \frac{1}{\xi^2 + a} d\xi = \begin{cases} \frac{1}{\sqrt{a}} \tan^{-1}\left(\frac{\xi}{\sqrt{a}}\right), & \text{for } a > 0 \\ -\frac{1}{\xi}, & \text{for } a = 0 \end{cases} \quad (B5c)$$

Substituting Eq. (B5) into Eq. (B4) and rearranging the terms, we obtain

$$I = \frac{1}{d_k} \left\{ A_{mij}(t_{k+1} - t_k) + \left[A_{mij} |\beta_1 y| - \frac{B_{mij} y(t_{k+1} - x - \alpha_1 y)}{|\beta_1 y|} \right] \right.$$

$$\times \left[\tan^{-1}\left(\frac{x - t_{k+1} + \alpha_1 y}{|\beta_1 y|}\right) - \tan^{-1}\left(\frac{x - t_k + \alpha_1 y}{|\beta_1 y|}\right) \right]$$

$$- \frac{A_{mij}(t_{k+1} - x - \alpha_1 y) + B_{mij} y}{2} \ln$$

$$\left. \times \left[\frac{(x - t_{k+1} + \alpha_1 y)^2 + \beta_1^2 y^2}{(x - t_k + \alpha_1 y)^2 + \beta_1^2 y^2} \right] \right\} \quad (B6)$$

The solution for the second integral in Eq. (B2) is the same as Eq. (B6) by replacing the material constants A_{mij} with C_{mij} and B_{mij} with D_{mij} .

References

- ¹Civelek, M. B., "Stress Intensity Factors for a System of Cracks in an Infinite Strip," *Fracture Mechanics, Sixteenth Symposium*, edited by M. F. Kanninen and A. T. Hopper, ASTM Special Technical Publ. 868, American Society for Testing and Materials, Philadelphia, 1985, pp. 7–26.
- ²Delale, F., Bakirta, I., and Erdogan, F., "The Problem of an Inclined Crack in an Orthotropic Strip," *Journal of Applied Mechanics*, Vol. 46, 1979, pp. 90–96.
- ³Suo, Z., and Hutchinson, J. W., "Interface Crack Between Two Elastic Layers," *International Journal of Fracture*, Vol. 43, 1990, pp. 1–18.
- ⁴Chandra, A., Hu, K. X., and Huang, Y., "A Hybrid BEM Formulation for Multiple Cracks in Orthotropic Elastic Components," *Computers and Structures*, Vol. 56, 1995, pp. 785–797.
- ⁵Jiang, Z. Q., Chandra, A., and Huang, Y., "A Hybrid Micro-Macro BEM with Micro-Scale Inclusion-Crack Interactions," *International Journal of Solids and Structures*, Vol. 33, 1996, pp. 2309–2329.
- ⁶Huang, H., and Kardomateas, G. A., "Single-Edge and Double-Edge Cracks in a Fully Anisotropic Strip," *Journal of Engineering Materials and Technology*, Vol. 121, 1999, pp. 422–429.
- ⁷Jagannadham, K., and Marcinkowski, M. J., "Surface Dislocation Model of a Finite Stressed Solid," *Materials Science and Engineering*, Vol. 38, 1979, pp. 259–270.
- ⁸Sheng, C. F., "Boundary Element Method by Dislocation Distribution," *Journal of Applied Mechanics*, Vol. 54, 1987, pp. 105–109.
- ⁹Theocaris, P. S., and Ioakimidis, N. I., "Numerical Integration Method for the Solution of Singular integral Equations," *Quarterly Applied Mathematics*, Vol. 35, 1977, pp. 173–183.
- ¹⁰Erdogan, F., and Gupta, G. D., "On the Numerical Solution of Singular Integral Equations," *Quarterly Applied Mathematics*, Vol. 30, 1972, pp. 525–534.
- ¹¹Cheung, Y. K., and Chen, Y. Z., "Solutions of Branch Crack Problems in Plane Elasticity by Using New Integral Equation Approach," *Engineering Fracture Mechanics*, Vol. 28, 1987, pp. 31–47.
- ¹²Zang, W., and Gudmundson, P., "An Integral Equation Method for Piece-Wise Smooth Cracks in an Elastic Half-Plane," *Engineering Fracture Mechanics*, Vol. 32, No. 6, 1989, pp. 889–897.
- ¹³Lee, J. C., "Analysis of a Fiber Bridged Crack Near a Free Surface in Ceramic Matrix Composites," *Engineering Fracture Mechanics*, Vol. 37, No. 1, 1990, pp. 209–219.
- ¹⁴Bueckner, H. F., "The Propagation of Cracks and the Energy of Elastic Deformation," *Journal of Applied Mechanics*, Vol. 30, No. 10, 1958, pp. 1289–1300.
- ¹⁵Hills, D. A., Kelly, P. A., Di, D. N., and Korsunsky, A. M., *Solution of Crack Problems; the Distributed Dislocation Technique*, Kluwer Academic, Norwell, MA, 1996.
- ¹⁶Atkinson, C., and Eftaxiopoulos, D. A., "Interaction Between a Crack and a Free or Welded Boundary in Media with Arbitrary Anisotropy," *International Journal of Fracture*, Vol. 50, 1991, pp. 159–182.
- ¹⁷Lekhnitskii, S. G., *Theory of Elasticity of an Anisotropic Body*, Mir Publishers, Moscow, 1963.

S. Saigal
Associate Editor

Economic Principles Applied to Space Industry Decisions

Joel S. Greenberg, Princeton Synergetics, Inc.



This is not an economics book. It is a book about the application of economic principles and concepts in decision making related to space activities. The book is primarily tutorial and elaborates upon concepts and methodology and their applications. Emphasis is placed upon applications with typical results of performed analyses presented to demonstrate concepts and methods.

The use of mathematical and simulation models serves as the underpinning for much of the presented materials. The specific models considered have been selected to demonstrate the role that a structured thought process can play in the decision process. Since most decisions relating to technology development, product design, capital expenditures, and investments involve uncertainty and risk, a number of the selected models, developed methodologies, and presented examples explicitly and quantitatively consider uncertainty and risk.

The objective of this book is to put economic analysis into perspective with respect to real-world decision making in the space industry. It will expand the perspective of the reader with respect to the type of tools and analyses that might be brought to bear on complex business and government problems.

Contents:

Introduction • Investment Decisions • RLV Economics • Space Operations • Licensing and Regulatory Issues • Beyond Space: Energy and Gaming • Appendix: Estimating the Likelihood of Investment

Progress in Astronautics and Aeronautics Series
2003, 480 pages, Hardback
ISBN: 1-56347-607-X
List Price: \$100.95
AIAA Member Price: \$69.95

Publications Customer Service, P.O. Box 960
Herndon, VA 20172-0960
Phone: 800/682-2422; 703/661-1595
Fax: 703/661-1501
E-mail: warehouse@aiaa.org • Web: www.aiaa.org